Scattering in a two-dimensional photonic crystal: An analytical model

T. J. Shepherd and P. J. Roberts
Defence Research Agency Malvern, St. Andrews Road, Malvern, Worcestershire WR14 3PS, United Kingdom
(Received 14 October 1994)

An exact analysis of light propagation in a model two-dimensional photonic crystal is presented. The system displays full and absolute band gaps in its dispersion characteristics. It is shown that global propagation of *s*-polarized light derives largely from locally evanescent waves.

PACS number(s): 41.20.Jb, 68.90.+g, 71.25.Tn

In this Brief Report we present a two-dimensional model of a periodic dielectric medium— a "photonic crystal"—from which physical quantities relating to electromagnetic propagation are analytically available. The model permits simple computation of the band structure, and displays full and absolute photonic band gaps.

Ever since the demonstration at microwave frequencies by Yablonovitch and co-workers [1] of the existence of the photonic band gap, many attempts have been made to understand the underlying behavior of the electromagnetic field in the presence of the periodic composite medium giving rise to the phenomenon. These studies have employed numerical methods, save for the analysis of one-dimensional periodicities, which can often be treated exactly [2]. Numerical methods include k-space expansions [3], transfer matrix techniques [4], and an electromagnetic form of the Korringa-Kohn-Rostinger (KKR) method [5].

The electronic analog of the two-component multilayer system was first investigated by Kronig and Penney [6]. In this one-dimensionally periodic system scattering is nondiffractive [7], and is thus analytically accessible. Kronig and Penney also outlined a three-dimensional version of this system that remained analytically tractable, thanks to the separability of the Schrödinger equation and the associated potential. Unfortunately, this separability does not automatically extend to the electromagnetic field for the corresponding dielectric distribution. Nevertheless, as we shall show, it is still possible to solve analytically for a related nondiffractive system.

The model we shall investigate is one in which the dielectric material consists of infinitesimally thick planes of infinite dielectric constant. Thus, for definiteness, we consider a dielectric slab of relative permittivity ε and thickness l, and define the dielectric parameter m such that $m=\varepsilon l$. Accordingly, we allow ε to go to infinity and l to go to zero, while m remains finite and fixed. This type of limit has been studied previously to model the dielectric interface between a Fabry-Perot cavity medium and the exterior to the cavity [8]. We assume a rectangular, two-dimensional periodicity such that the inhomogeneous relative dielectric constant takes the form

$$\varepsilon(\mathbf{r})=1+m\left[\sum_{n_2=-\infty}^{\infty}\delta(x_2-n_2a)+\sum_{n_3=-\infty}^{\infty}\delta(x_3-n_3a)\right],$$

with $\mathbf{r}=(x_1,x_2,x_3)$ and where a is the spacing between successive dielectric sheets. (The scalar counterpart to this system, for electrons, was alluded to in the original work by Kronig and Penney [6]. A detailed exposition of the three-dimensional version of their model has been given in the thesis by Angus [9], and alternative geometries were explored by Sutherland [7,10].) The system can approximate a structure consisting of cylindrical free-space voids in a dielectric material of infinite extent.

It can be shown from Maxwell's equations that the field discontinuities across each planar interface are given by

$$\Delta\mathbf{H}=-m\varepsilon_0\mathbf{n}\times\frac{\partial\mathbf{E}}{\partial t}\ , \tag{1}$$

$$\Delta\mathbf{E}=-m\mathbf{n}(\mathbf{n}\times\nabla)\cdot(\mathbf{n}\times\mathbf{E})\ , \tag{2}$$

where $\Delta\mathbf{E}$ and $\Delta\mathbf{H}$ are the increments in the electric and magnetic fields $\mathbf{E}$ and $\mathbf{H}$, respectively. ε_0 is the permittivity of free space, and $\mathbf{n}$ is a unit vector, normal to the interface, pointing in the direction of the field increment. A free-space region is assumed on either side of the dielectric plane.

In the following all fields oscillate with a time dependence of $e^{-i\omega t}$, and we consider only propagation within the x_2-x_3 plane. For this two-dimensional propagation the fields decompose into *s*-polarized states (electric field vector parallel to dielectric sheets) and *p*-polarized states (magnetic field vector parallel to dielectric sheets).

For *s*-polarized light, we choose

$$k_1=0\quad(k_2^2+k_3^2=k^2=\omega^2/c^2)\ . \tag{3}$$

The electric field is given by

$$\mathbf{E}(\mathbf{r})=(E_1(\mathbf{r}),0,0)$$

with $E_1(\mathbf{r})$ expanded as

$$E_1(\mathbf{r})=(E_{1,2}^{(+)}e^{ik_2x_2}+E_{1,2}^{(-)}e^{-ik_2x_2})\times(E_{1,3}^{(+)}e^{ik_3x_3}+E_{1,3}^{(-)}e^{-ik_3x_3})\ .$$

The corresponding magnetic field can then be found from the Maxwell equation $\nabla\times\mathbf{E}=i\omega\mu_0\mathbf{H}$, where μ_0 is the permeability of free space.

Application of the boundary conditions (1) and (2) across the plane at $x_3=0$ relates the field coefficients $E_{1,i}^{(\pm)}$ $(i=2,3)$ as follows:

$$T_s(\mathbf{k})E^{(a)}=KE^{(b)}\ , \tag{4}$$

where $E^{(a)}$ represents either of the vectors

$$E=\begin{bmatrix} E_{1,2}^{(+)}E_{1,3}^{(+)} \\ E_{1,2}^{(+)}E_{1,3}^{(-)} \end{bmatrix}, \quad \begin{bmatrix} E_{1,2}^{(-)}E_{1,3}^{(+)} \\ E_{1,2}^{(-)}E_{1,3}^{(-)} \end{bmatrix}$$

and the superscript (a) and (b) distinguishes the fields on either side of the plane; the field labeled by (b) is defined to be on the side into which $\mathbf{n}$ points. The matrices $T_s(\mathbf{k})$ and K are defined by

$$T_s(\mathbf{k})=\begin{bmatrix} 1 & 1 \\ (1+imk^2/k_3) & (-1+imk^2/k_3) \end{bmatrix}$$

and

$$K=\begin{bmatrix} 1 & 1 \\ 1 & -1 \end{bmatrix}.$$

p-polarized light is characterized in a similar way in terms of the magnetic field, and results in the p-polarization counterpart to $T_s(\mathbf{k})$:

$$T_p(\mathbf{k})=\begin{bmatrix} (1+imk_3) & (1-imk_3) \\ 1 & -1 \end{bmatrix}.$$

The boundary conditions above can also be carried over to relating free-space fields separated by sheets in the parallel x_1-x_3 planes.

Stable propagation through an infinite periodic medium is characterized by the Bloch wave vector $\boldsymbol{\mu}$: According to Bloch's theorem, fields separated by a lattice vector $\mathbf{R}$ are related by

$$\mathbf{E}_{\mu}(\mathbf{r}+\mathbf{R})=e^{i\boldsymbol{\mu}\cdot\mathbf{R}}\mathbf{E}_{\mu}(\mathbf{r}) .$$

A similar relation applies to the magnetic field $\mathbf{H}(\mathbf{r})$. Combining these with Eq. (4) and its magnetic field counterpart, applied in both the x_2 and x_3 directions, we obtain the consistency equations: for s polarization,

$$\cos(\mu_i a)=\cos(k_i a)-(mk^2/2k_i)\sin(k_i a) \quad (i=2,3) , \tag{5}$$

and for p polarization,

$$\cos(\mu_i a)=\cos(k_i a)-(mk_i/2)\sin(k_i a) \quad (i=2,3) . \tag{6}$$

Each of Eqs. (5) and (6) for the wave vectors μ_i and k_i is identical in form to the dispersion relation for normal propagation in a one-dimensional arrangement of dielectric sheets distributed in the x_i direction. The combination here, however, of the x_2 and x_3 components, together with the free-space dispersion relation (3), gives rise to complex dynamics peculiar to two-dimensional propagation.

With the local wave vector parametrized as $\mathbf{k}=(0,\sin\theta,\cos\theta)\omega/c$, constant-frequency dispersion curves for p-polarized light may be obtained from Eqs. (6). Figure 1 depicts a series of two-dimensional curves in one quarter of the square Brillouin zone. The coordinates of each point are $(\mu_2 a/\pi,\mu_3 a/\pi)$, with θ in the range $0\le\theta<\pi/2$, and for $m/2a=1$. We may define $\omega'=\omega a/c$, and label symmetry points and axes as shown in the inset in Fig. 3. Figure 1(a) shows curves for ω' in the range 0–1.8. The initial low-frequency, long-wavelength behavior is apparent in the near-circular contours. At higher frequencies, Bragg reflection begins to take effect from $\omega'=1.4$. Beyond $\omega'=1.8$ there are no contours until $\omega'=3.2$, the contours for which are shown in Fig. 1(b); there is thus a complete band gap for p-polarized light between $\omega'=1.8$ and 3.2. Figure 1(b) displays contours of ω' from 3.2 to 3.8, above which the next gap occurs. Equations (6) dictate that the constant-frequency contours be symmetrical about the Σ line. This implies that *asymmetrical* contours must exist with a partner contour formed by reflection in Σ. The two contours cross on the diagonal and give rise to a degenerate mode in the Σ direction.

Figure 2 shows curves of constant frequency for s polarization, computed from Eqs. (5). In this instance, however, scanning over the range $0\le\theta<\pi/2$ merely produces the solid curves which do not extend over all Bloch wave-vector angles. In Eqs. (5) it is seen that even for low frequencies neither $\mu_2 a/\pi$ nor $\mu_3 a/\pi$ vanishes when θ takes the value 0 or $\pi/2$. This implies that Bloch wave propagation can occur in directions oblique to the dielectric planes even though the local wave vector $\mathbf{k}$ is parallel to one set of planes. At this angle the singular behavior of the s-polarization transfer matrix $T_s(\mathbf{k})$ as k_2 or k_3 goes to zero may be traced to the vanishing of one component of the tangential magnetic field. This is a purely

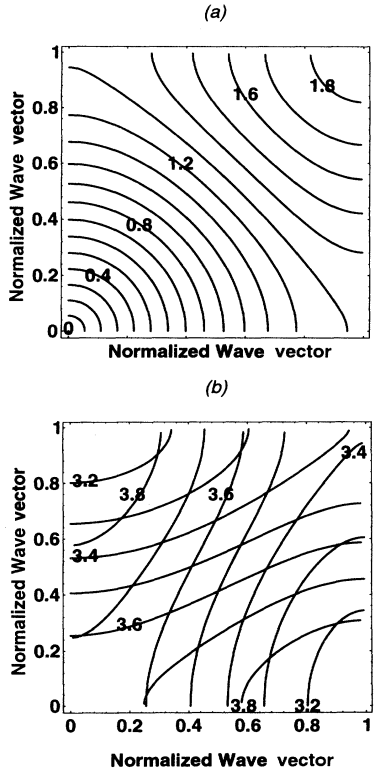

FIG. 1. Constant-frequency contours for p-polarized light in the positive quadrant of the square lattice Brillouin zone. Frequencies shown on each contour are in units of c/a, and normalized wave vectors in units of π/a. (a) Contours for the lowest band. (b) Contours for the second band.

geometrical effect, but has the consequence that the electric field must also vanish in this limit. The reason for this follows from consideration of simple reflection into free space from any dielectric planar interface. For s-polarized light, the Fresnel equations predict a phase change of π radians in the electric field upon reflection; they also predict that the amplitude of the reflected wave approaches that of the incident wave in the limit of glancing incidence, at which point the two waves interfere destructively.

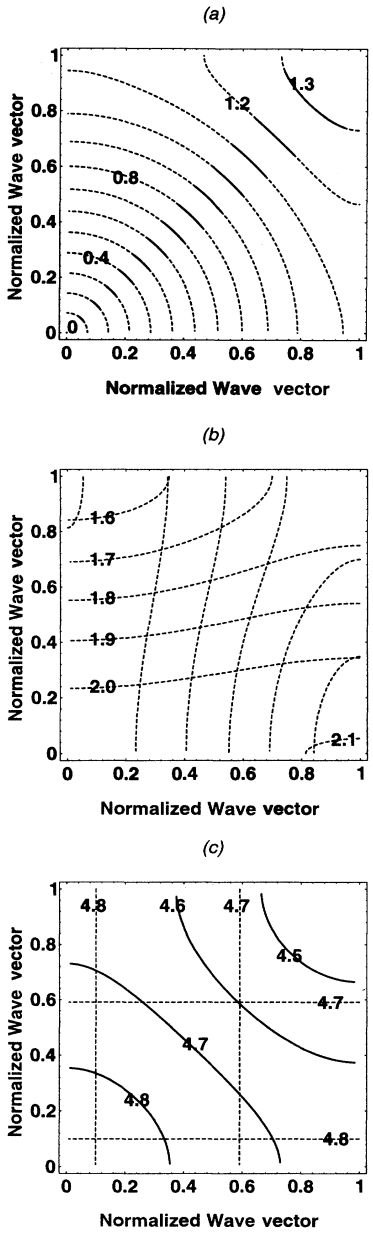

FIG. 2. Constant-frequency contours for s-polarized light. Units are as in Fig. 1. Solid lines denote that Bloch wave propagation derives from propagating local modes, and dashed lines signify evanescent local modes. (a) Contours for the lowest band. (b) Contours for the second band. For this and the subsequent five bands Bloch wave propagation is due entirely to evanescent local waves. (c) Contours for the eighth band. Both evanescent and propagating local modes contribute to Bloch waves.

We now consider *evanescent* local modes, for which the local wave vector becomes imaginary. Specifically, we take $k_3 > \omega/c$, and k_2 imaginary. The local vector $\mathbf{k}$ is parametrized now as $\mathbf{k}=(0,\ i\sinh\alpha,\ \cosh\alpha)\omega/c$. This procedure can be repeated, interchanging k_2 and k_3. The resulting curves are represented by the dashed lines in Fig. 2. It is seen that real local wave propagation dies out for frequencies above the band gap between $\omega'=1.3$ and 1.6. Above this frequency, all global propagation for s-polarized light occurs as a result of local evanescent waves until the frequency $\omega'=4.7$, at which a locally propagating mode appears, shown as the solid curve in Fig. 2(c). The existence of evanescent modes signals the presence of trapped (waveguide) modes within a high dielectric region. Indeed, it is possible to show that an isolated dielectric sheet can harbor a single trapped mode—for s polarization only—with an external evanescent field decaying over a length $2c^2/(m\omega^2)$.

The dispersion curves are computed from Eqs. (5) and (6), upon setting μ_2 and μ_3 to the appropriate value for the given line, and solving the equation for θ. In principle this must be done for each value of ω'. For the case of p polarization, however, setting μ_2' or μ_3' to zero provides analytical dispersion expressions for *all* frequencies. (These solutions correspond to more than just the values 0 or $\pi/2$ for θ, that are associated with purely one-dimensional periodicity.) Corresponding dispersion relations for both p- and s-polarized light are shown in Fig. 3. The degeneracies noted above are apparent for both polarizations in the Σ direction. Nearly all s-polarization bands derive from evanescent local waves: the band originating from propagating local waves, evident in Fig. 2(c), appears between ω' of 4.6 and 4.8. Full (for all direction in the plane) and absolute (for both polarizations) band gaps occur around ω' values of 2.2, 2.8, and 4.2 in the

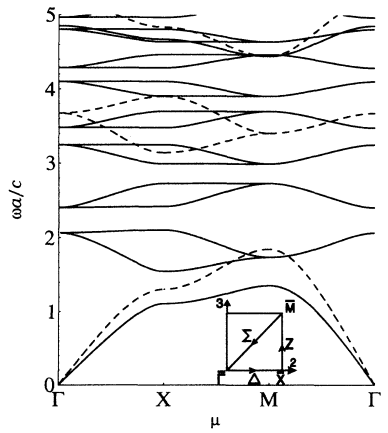

FIG. 3. Dispersion curves: s-polarization components (solid lines) and p-polarization (dashed lines). Frequencies (ordinate axis) are shown in units of c/a. Symmetry points Γ, X, and M in the Brillouin zone (inset) are at Bloch wave-vector (abscissa axis) values of $\mu=\pi/a$ times [0,0], [0,1], and [1,1], respectively. The $M\Gamma$ interval is scaled down by a factor of $\sqrt{2}$.

figure. (The band edges can be analytically determined.) It is also possible to show that in the long-wavelength limit the *s*- and *p*-polarized components have effective refractive indices of $\sqrt{1+2m/a}$, and $\sqrt{1+m/a}$, respectively. Interestingly, these values correspond respectively to the space-averaged permittivities of the two- and one-dimensional periodic media.

Treatment of this simple model can be extended in several ways: more general geometries, (e.g., triangular or hexagonal) in which the field conforms to that of the Bethe Ansatz [10,11]; propagation in three dimensions; computation of densities of states. These issues will be addressed in a future publication. In conclusion, the model constitutes a useful analytical "laboratory" in which to test the properties of more general photonic crystals.

The authors thank Professor R. Loudon, Professor E. Jakeman, and Dr. P. St. J. Russell for many helpful discussions and suggestions, and Professor Bill Sutherland for information on the relevant literature. They are also very grateful to Dr. R. Kennedy Angus for giving permission to copy and quote his thesis. This work was supported by the UK Ministry of Defence Strategic Research Programme.

[1] E. Yablonovitch, T. J. Gmitter, and K. M. Leung, Phys. Rev. Lett. **67**, 2295 (1991); E. Yablonovitch, T. J. Gmitter, R. D. Meade, A. M. Rappe, K. D. Brommer, and J. D. Joannopoulos, *ibid.* **67**, 3380 (1991).

[2] P. Yeh, *Optical Waves in Layered Media* (Wiley, Interscience, New York, 1988).

[3] K. M. Leung, and Y. F. Liu, Phys. Rev. Lett. **65**, 2646 (1991); Z. Zhang and S. Satpathy, *ibid.* **65**, 2650 (1991); K. M. Ho, C. T. Chan, and C. M. Soukoulis, *ibid.* **65**, 3152 (1991).

[4] J. B. Pendry and A. MacKinnon, Phys. Rev. Lett. **69**, 2772 (1992).

[5] N. Stefanou, V. Karathanos, and A. Modinos, J. Phys. Condens. Matter **4**, 7389 (1992).

[6] R. de L. Kronig and W. G. Penney, Proc. R. Soc. London Ser. A **130**, 499 (1931).

[7] B. Sutherland, J. Math. Phys. **21**, 1770 (1980).

[8] R. Lang, M. O. Scully, and W. E. Lamb, Phys. Rev. A **7**, 1788 (1973); B. Baseia and H. M. Nussenzweig, Opt. Acta **31**, 39 (1984); J. C. Penaforte and B. Baseia, Phys. Rev. A **30**, 1401 (1984); Phys. Lett. **107A**, 250 (1985); M. Ley and R. Loudon, J. Mod. Opt. **34**, 227 (1987).

[9] R. K. Angus, D. Phil. thesis, University of Oxford, 1959.

[10] B. Sutherland, Phys. Rev. Lett. **42**, 915 (1979).

[11] M. Gaudin, *La Fonction d'Onde de Bethe* (Masson, Paris, 1983).